THE APPLICABILITY OF A 5–18 μm ARRAY CAMERA TO SOLAR IMAGING

DANIEL Y. GEZARI

NASA/Goddard Space Flight Center, Infrared Astrophysics Branch, Code 685, Greenbelt, MD 20771, U.S.A.

Abstract. The anticipated requirements and operating conditions are considered for using a mid-infrared array camera in broad- and narrow-band solar imaging observations. The array camera system was designed for high-background 5–18 μm general astronomical imaging observations. The electronic and optical design of the camera, its photometric characteristics, examples of observational results, and the requirements for imaging in both high- and low-background solar applications are discussed.

Key words: infrared: general – instrumentation: detectors – Sun: general

1. Introduction

Solar imaging with an array camera at mid-infrared (5–20 μm) wavelengths introduces quite a different a set of concerns and requirements from those of either conventional infrared photometry or infrared array imaging observations of stellar sources. These include the problems of dealing with 1) high source signal levels in addition to the large 10 μm thermal background from the telescope optics and sky, 2) spatial chopping for background subtraction when observing a very extended source, 3) precise pointing, guiding and registration of images using an instrument capable of very high spatial resolution ($\sim$1″) and relative astrometric precision ($\sim$0.1″), and 4) assembling mosaic images from individual exposures of extended, low contrast infrared surface features which may not have visible counterparts.

In a $T \sim 270$ K observatory environment, the 10-μm thermal background photon flux in the Cassegrain focal plane of a large ($\sim$3 m) conventional telescope is about 10^9 photon s^{-1} m^{-2} μm^{-1} $arcsec^{-2}$, while the detector well capacity of infrared photoconductor arrays is typically 10^5–10^6 electrons. However, the small detector pixels, the optical efficiency of the camera instrument, the low photoconductive gain at which the detector can be operated, and the reasonably short integration time combine to reduce the number of electrons which actually accumulate in each detector well during an integration by about four orders of magnitude, making operation of the large-format array feasible.

2. The Array Camera Instrument

The infrared array camera system described here was developed for general high-background, diffraction-limited 5–18 μm astronomical imaging on large optical telescopes. The camera uses a 58 × 62 pixel Si:Ga (gallium doped silicon) photoconductor array detector manufactured by Hughes/Santa Barbara Research Center (SBRC). A full discussion of the array detector characteristics, camera optical and electronic design, and operating strategy has been presented by Gezari *et al.* (1992).

The detector array is a hybrid device, assembled from a wafer of Si:Ga detector material (nominally sensitive from 5–17 μm), bump-bonded to a Hughes CRC-228

D. M. Rabin et al. (eds.), Infrared Solar Physics, 595–601.

https://doi.org/10.1017/S0074180900124891 Published online by Cambridge University Press

direct readout (DRO) integrated circuit multiplexer chip (Hoffman 1987). The array pixels are read out serially, although the switched FET multiplexer design allows them to be sampled in any order, or polled non-destructively to determine the fullness of the well in low-signal, low-background applications (with the penalty only of added read noise). In the case of this Si:Ga photoconductor array, the photoconductive gain of the detector, G_{pc}, is a function of net detector bias. G_{pc} can be reduced to about 0.1 by operating at a net detector bias of 4 volts. Since G_{pc} is a post-detection gain factor, reducing the photoconductive gain reduces the number of electrons generated per incident photon, but does not change the incident photon statistics or signal/noise of the observation. This characteristic of the device permits broad-band operation of the array at higher backgrounds, with better relative photon noise statistics.

The camera front-end electronics (Folz 1989) includes dual low-noise preamp modules, a regulated low-noise bias power supply, dual high-speed A/D converters, array clocking and pixel address timing generator, and a detector temperature monitor/regulator. Two 16-bit Analogics Corp. ADAM 826-1 analog-to-digital converter modules are used which can operate at 3 μs per conversion, permitting the camera frame rate to be limited by the intrinsic time constants of the array detector multiplexer. A Mercury ZIP-3216 array processor residing on the Q-bus of the DEC LSI-11/73 host computer system is used to acquire and co-add digital data from the A/D converters. The incoming image data from the two positions of the telescope chopping secondary mirror are sorted into two arrays by the ZIP, synchronized with the chopper drive signal. Data are ignored while the chopper mirror is moving between end positions. Two final images (source and sky) are down loaded to the LSI 11/73 host computer for image pair storage.

The camera optical design (Gezari 1989) uses a single off-axis parabolic mirror and a cold aperture stop (Fig. 1), providing achromatic performance, simple optical alignment, diffraction-limited images, and good suppression of out-of- field background radiation. The array plate scale is $0.26''$ pixel^{-1}, a field-of-view of $15.0'' \times 16.1''$ on the 3.0-m, $f/35$ NASA Infrared Telescope Facility (IRTF) on Mauna Kea. The camera optics are diffraction-limited at wavelengths $\lambda > 5$ μm and typically produce $1.0 \pm 0.1''$ seeing- and tracking-limited stellar images in long integrations on the IRTF. Aberrations and distortion (pincushion, *etc.*) and field rotation are negligible, less than 1/2 pixel across the full field of the array (corresponding to $< 0.5°$ of field rotation). Two filter wheels contain a 4.8–14.0 μm, OCLI-Corp. circular variable filter (CVF), a set of OCLI-Corp. fixed interference filters (Silicate Filter Set) at 7.8, 8.7, 9.8, 10.3, 11.6 and 12.4 μm, and a set of neutral density filters for laboratory test work. The spectral bandwidth of the CVF is $\Delta\lambda/\lambda = 0.04$ at 10 μm (defined by the width of the cold aperture stop) with ~50% transmission. The fixed filters have $\Delta\lambda/\lambda = 0.1$ bandwidths and ~80% transmission. The combined instrumental optical efficiency is about 0.5 with the fixed filters, and is reduced to ~0.3 using the CVF. An 18.1-μm fixed interference filter is also installed, and the camera operates with ~50% efficiency beyond the nominal cut-off of the the Si:Ga detector, in a narrow spectral region between the cut-on of the 20 μm (Q band) atmospheric window at about 17 μm and the exponential fall-off of the Si:Ga detector quantum efficiency longward of 18 μm.

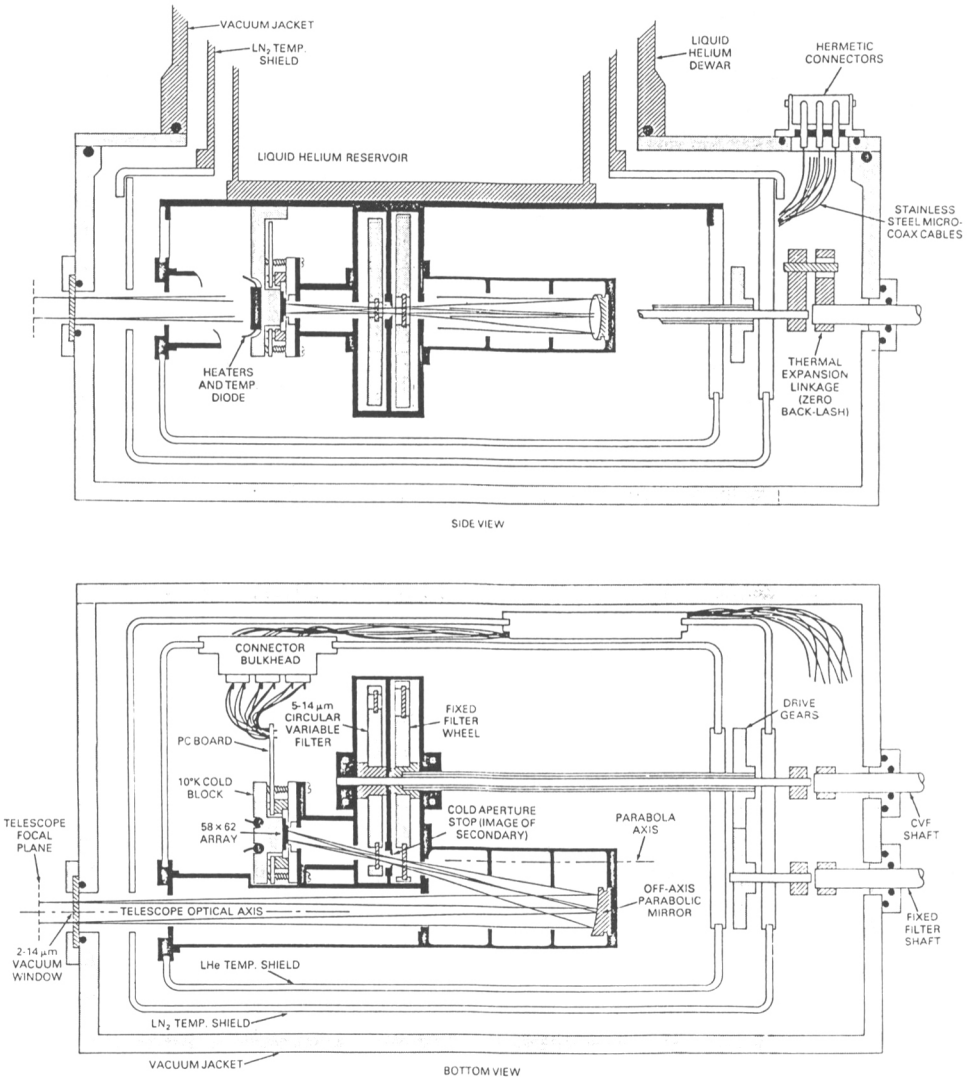

Fig. 1. Optical design and mechanical layout of the cryogenic dewar optical bench, showing the arrangement of the off-axis parabola, cold aperture stop at the image of the telescope secondary mirror, and the array at the de-magnified image of the telescope focal plane. The cold optics are surrounded by an optical baffle system at LHe temperature, within the outer LHe temperature radiation shield, to minimize light leaks.

https://doi.org/10.1017/S0074180900124891 Published online by Cambridge University Press

The observational noise equivalent flux density (NEFD) on the IRTF using the relatively narrow-bandwidth CVF filter ($\Delta\lambda/\lambda = 0.04$, transmission ~ 0.5) at 10 μm is

$$\mathrm{NEFD}(1\sigma) \approx 0.03 \text{ Jy pixel}^{-1}\text{min}^{-1/2},$$

(1 Jy $\equiv 1.0 \times 10^{-26}$ W m^{-2} Hz^{-1}). However, the more efficient fixed interference filters ($\Delta\lambda/\lambda = 0.1$, transmission ~ 0.8) are used for most observations, and the improved photon statistics due to the increased bandwidth and transmission result in

$$\mathrm{NEFD}(1\sigma) = 0.010 \text{ Jy pixel}^{-1}\text{min}^{-1/2}$$

with the fixed filters, corresponding to a noise equivalent brightness

$$\mathrm{NEB} = 0.15 \text{ Jy min}^{-1/2}\text{arcsec}^{-2}$$

(the surface brightness of an extended source yielding a 1σ detection). The image contrast we can detect in the background-limited image is about one part in 10^4.

3. Observational Considerations for Infrared Solar Imaging

In non-solar broadband ground-based applications at 10 μm, thermal background radiation completely dominates the incident photon flux. In most cases the raw image of an astronomical source (*i.e.*, the image before background subtraction) is indistinguishable from a raw image of blank sky (see Fig. 2). Blank sky images observed simultaneously using the telescope chopping-secondary mirror are used for precise background subtraction. The background flux can have both a temporal and spatial dependence. At present, slow ($\sim$1 Hz) chopping is standard procedure for high background observations at thermal infrared wavelengths. *In principle*, chopping should not be required for sky subtraction or flat-fielding of high-background array image data. Sky background subtraction could be done without chopping if some part of an image were known to contain blank sky or a well-defined signal level, and an accurate gain-matrix existed for that image. In practice, temporal variations in the sky flux level on a $\sim$10 s time-scale make spatial chopping a basic part of the current operating procedure. Background subtraction, chopping and flat-fielding techniques are discussed in detail by Gezari *et al.* (1992).

A broadband mid-infrared observation of the Sun is not necessarily a "high background" measurement. The incident flux from the solar surface with $\Delta\lambda/\lambda \sim 1$ would saturate the array camera in its normal configuration by a factor of roughly 1,000. To cope with this large signal would require the use of either a cold neutral density filter inside the dewar, a faster readout rate, use of only a portion of the full array, or some combination of the three. Technically this is an inefficient observing mode since signal/noise is reduced, but is acceptable if narrowing the spectral bandpass is undesirable for scientific reasons (or simply impractical), especially since the Sun is such a strong infrared source. The observer pays no real penalty, because of the large relative continuum signal. The environmental background detected using a cold neutral density filter would be negligible compared to the solar flux in such a broadband observation, and could be thought of as a "low background" measurement. This observation might well be successful without spatial chopping for background subtraction (discussed below).

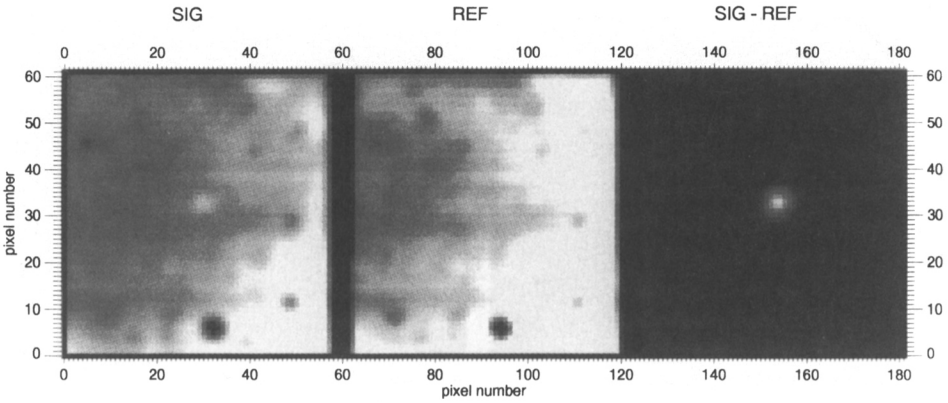

Fig. 2. The individual raw source (SIG) and reference (REF) images of the bright star α Boo, and the final sky-subtracted image (SIG - REF) obtained by taking the difference between the two. The star can barely be seen above the background in the SIG image. A gain gradient of about 30% can be seen across the field. Array gain defects of up to 25% of the mean can be seen resulting from defective bump-bonds. The gain variation over all of the pixels is 15% (1σ). Despite these gain non-uniformities, the sky-subtracted images can be flat-fielded to better than 0.015% (1σ) of the raw mean. Slight differences in the SIG and REF images shown here are due to the auto-ranging color display; the actual images appear essentially identical. If these image differences were real (due to sky background changes, *etc.*) the final sky-subtracted image would be useless.

Broadband observations of coronal structure would not require cold neutral density filters to attenuate the signal, and would thus fall into the "high background" category. However, in this case identifying a suitable featureless field-of-view to chop against (within a few arcmin of the observed position) for background subtraction might be a problem, as well might be scattered light from the nearby solar disk.

On the other hand, narrow bandwidth ($\Delta\lambda/\lambda < 10^{-3}$) imaging of solar surface features could be either a high background or low background observation, depending on whether the dispersing instrument is warm (an observatory facility spectrograph, for example) or cold (cooled spectrograph or Fabry-Perot cryogenically coupled directly to the array camera dewar). Using a cold dispersing instrument would dramatically improve the signal/noise ratio, and in this case the measurement would be read-noise- rather than background-limited. A narrow-band spectral line observation using a warm dispersing instrument would be a standard high-background measurement, with sensitivity limited by the noise level in the background from the warm instrument.

The environmental 10 μm background anticipated at the McMath Solar Telescope on Kitt Peak (altitude 2,100 m) can be compared to the 3-m Infrared Telescope Facility (IRTF) on Mauna Kea (altitude 4,200 m). Other things being equal, differences in ambient temperature (300 K *vs.* 270 K) and atmospheric precipitable water vapor (1 mm *vs.* ~3 mm in good weather) would combine to roughly double

https://doi.org/10.1017/S0074180900124891 Published online by Cambridge University Press

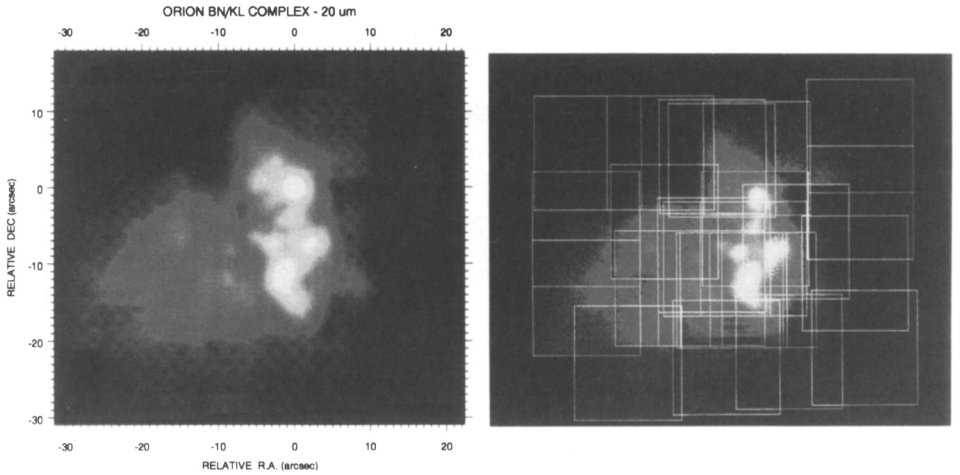

Fig. 3. 20-μm continuum mosaic of the Orion BN/KL complex obtained with the 58 × 62 array camera (Gezari *et al.* 1992) at the 3-m NASA IRTF Telescope on Mauna Kea. The mosaic was assembled from 23 overlapping 1-minute-integration frames (15″ × 16″ field of view, pixel size 0.26″) which were aligned, matched and co-added to make up the final mosaic, using our MOSAIC software package.

the 10 μm background at the McMath compared to the IRTF. But the slower focal ratio of the McMath (f/54 *vs.* f/35) would reduce the solid angle of warm telescope optics and sky seen by the array camera to 0.4 of that on the IRTF. The net result is that the 10 μm thermal background detected by the array camera at the two telescopes (with an appropriate change of cold aperture stop in the camera optics) should be roughly comparable. The array field of view on the McMath main beam would be 20″, corresponding to 0.33″ pixels, fully sampling the diffraction limited image at 10 μm (θ = 1.6″ FWHM).

An example of the array camera imaging results on an extended source is given here to illustrate how large mosaic images of complex fields can be assembled successfully from many individual overlapping array images. Figure 3 shows the Orion BN/KL complex at 20 μm. The data were reduced and this mosaic was made using the MOSAIC image analysis software package we have developed in IDL (Varosi and Gezari 1992).

Several factors combine to make array camera observations more difficult than first impressions might suggest. NEFD *per pixel* numbers can seem deceptively good, but this is because the array pixels are small. One should look at the values of the NEFD *per square arcsec* for a more realistic picture. The NEFD is expressed as the 1σ noise level, but good images require ~5σ results in most of the image, increasing integration time by 1–2 orders of magnitude over the NEFD time scale. Also, chopping more than doubles the elapsed observing time; overhead must be allowed for calibration observations; and flat fields (blank sky images for calibration) generally have to be observed to the same noise level as the image data. De-

https://doi.org/10.1017/S0074180900124891 Published online by Cambridge University Press

spite these burdens, infrared array cameras can make simultaneous, well sampled, high-spatial-resolution images of low-contrast solar surface features in a reasonable period of time, which would be completely impractical to attempt by mapping with a single detector bolometer system.

Acknowledgements

We are grateful to Mary Hewitt of Hughes/Santa Barbara Research Center (SBRC) for her expert guidance and her extraordinary generosity during the development of the array camera system. This research is funded by NASA/OSSA (RTOP 188-44-23-08) and the NASA/Goddard Director's Discretionary Fund.

References

Folz, W.: 1989, NASA Internal Document (preprint).
Gezari, D. Y.: 1989, NASA Internal Document (preprint).
Gezari, D. Y., Backman, D. Werner, M. W., McKelvey, M., and McCreight, C.: 1992, *Pub. Astron. Soc. Pacific*, in preparation.
Gezari, D. Y., Folz, W. C., Woods, L. A., and Varosi, F.: 1992, *Pub. Astron. Soc. Pacific* **104**, 191.
Hoffman, A. W.: 1987, in C. G. Wynn-Williams and E. E. Becklin (eds.), *Infrared Astronomy with Arrays*, University of Hawaii Press, p. 29.
Varosi, F. and Gezari, D. Y.: 1992, in preparation.